



NLO QCD OBSERVABLES IN 4D THROUGH THE LOOP-TREE DUALITY

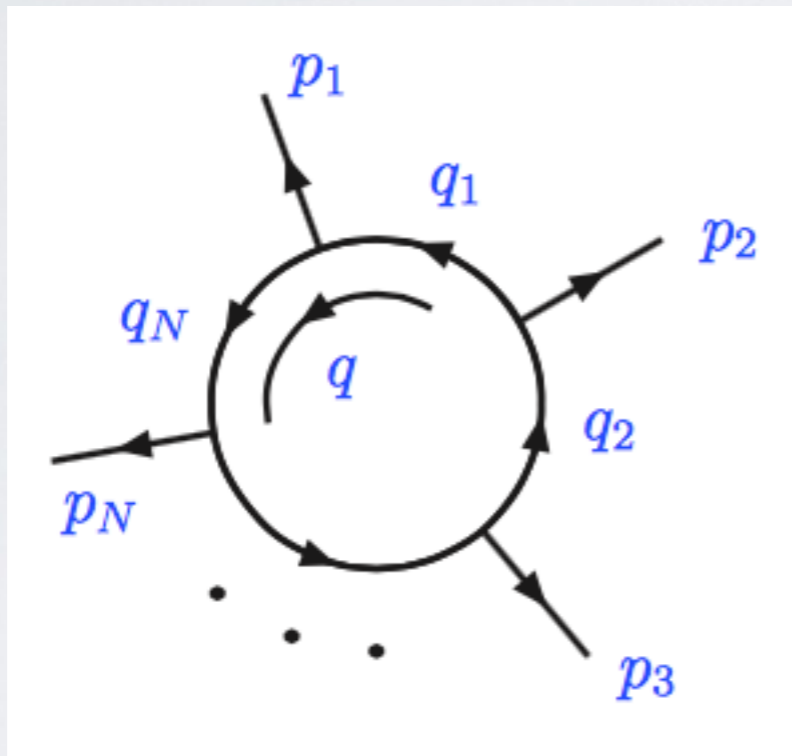
Roger J. Hernández Pinto
Facultad de Ciencias Físico-Matemáticas,
Universidad Autónoma de Sinaloa

in collaboration with: F. Driencourt-Mangin, G. F. R. Sborlini and G. Rodrigo

Reunión General de la Red FAE
Pachuca, Hidalgo, November 10th, 2016

LOOP-TREE DUALITY

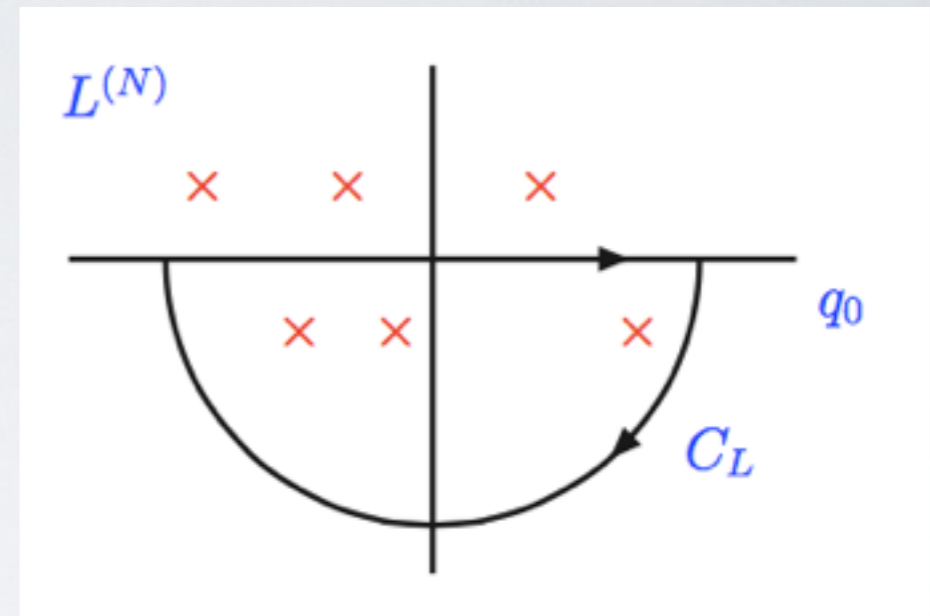
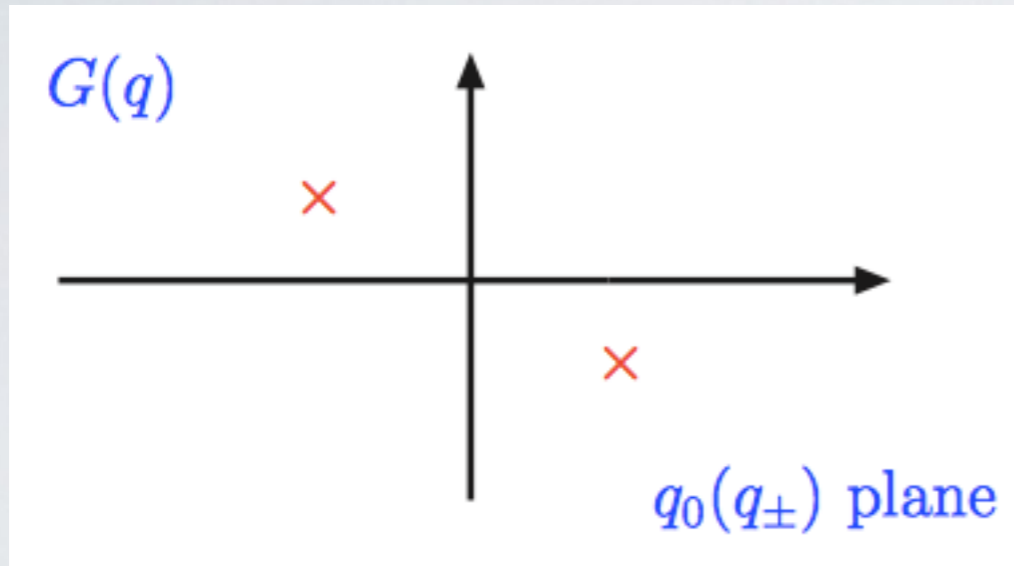
- Massive one-loop scalar integrals are,



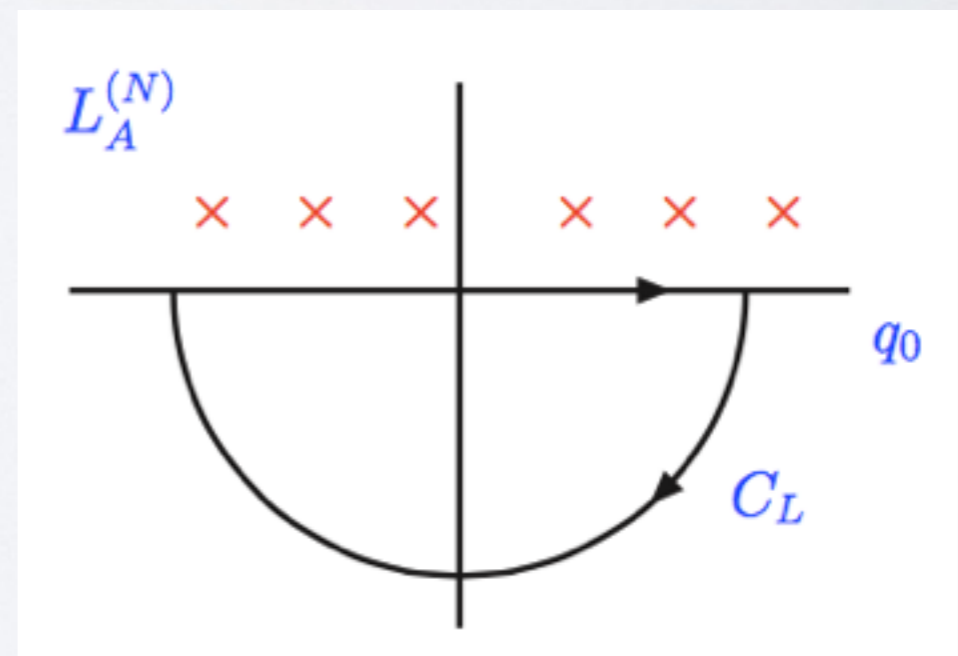
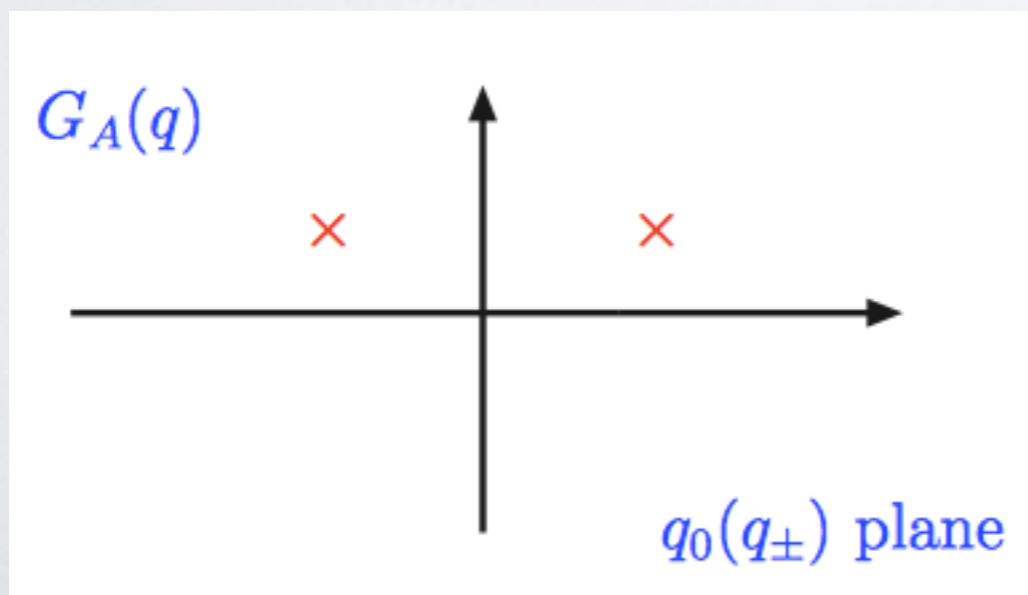
$$= -i \int \frac{d^d q}{(2\pi)^d} \prod_{i=1}^N \frac{1}{q_i^2 - m_i^2 + i0}$$

- where the $+i0$ prescription establishes that particles are going forward in time.

- The solution of the integrals are known by the Cauchy residues theorem.



- However, by using advanced propagators,



- LTD at one loop establishes then

$$L^{(1)}(p_1, \dots, p_N) = - \sum \int_{\ell_1} \tilde{\delta}(q_i) \prod_{\substack{j=1 \\ j \neq i}}^N G_D(q_i; q_j)$$

- where Feynman propagators are transformed to dual propagators.

$$G_D(q_i; q_j) = \frac{1}{q_j^2 - m_j^2 - i0\eta \cdot (q_j - q_i)}$$

- $\tilde{\delta}(q_i) = 2\pi i \theta(q_{i,0}) \delta(q_i^2 - m_i^2)$ and sets internal lines on-shell and in the positive energy mode.
- LTD modify the $+i0$ prescription, instead of having multiple cuts like in the Feynman Tree Theorem.
- η^μ is a future-like vector, for simplicity we take $\eta^\mu = (1, \mathbf{0})$. In fact, the only relevance is the sign in the prescription.

NUMERICAL IMPLEMENTATION

- Faster computations are needed for the Montecarlo simulations for the LHC observables.
- Using LTD the standard methods become time consuming
- (S. Buchta, et al. , arXiv:1510.00187)

	Rank	Tensor Pentagon	Real Part	Imaginary Part	Time [s]
P16	2	LoopTools	-1.86472×10^{-8}		
		SecDec	$-1.86471(2) \times 10^{-8}$		45
		LTD	$-1.86462(26) \times 10^{-8}$		1
P17	3	LoopTools	1.74828×10^{-3}		
		SecDec	$1.74828(17) \times 10^{-3}$		550
		LTD	$1.74808(283) \times 10^{-3}$		1
P18	2	LoopTools	-1.68298×10^{-6}	$+i 1.98303 \times 10^{-6}$	
		SecDec	$-1.68307(56) \times 10^{-6}$	$+i 1.98279(90) \times 10^{-6}$	66
		LTD	$-1.68298(74) \times 10^{-6}$	$+i 1.98299(74) \times 10^{-6}$	36
P19	3	LoopTools	-8.34718×10^{-2}	$+i 1.10217 \times 10^{-2}$	
		SecDec	$-8.33284(829) \times 10^{-2}$	$+i 1.10232(107) \times 10^{-2}$	1501
		LTD	$-8.34829(757) \times 10^{-2}$	$+i 1.10119(757) \times 10^{-2}$	38

	Rank	Tensor Hexagon	Real Part	Imaginary Part	Time[s]
P20	1	SecDec	$-1.21585(12) \times 10^{-15}$		36
		LTD	$-1.21552(354) \times 10^{-15}$		6
P21	3	SecDec	$4.46117(37) \times 10^{-9}$		5498
		LTD	$4.461369(3) \times 10^{-9}$		11
P22	1	SecDec	$1.01359(23) \times 10^{-15}$	$+i 2.68657(26) \times 10^{-15}$	33
		LTD	$1.01345(130) \times 10^{-15}$	$+i 2.68633(130) \times 10^{-15}$	72
P23	2	SecDec	$2.45315(24) \times 10^{-12}$	$-i 2.06087(20) \times 10^{-12}$	337
		LTD	$2.45273(727) \times 10^{-12}$	$-i 2.06202(727) \times 10^{-12}$	75
P24	3	SecDec	$-2.07531(19) \times 10^{-6}$	$+i 6.97158(56) \times 10^{-7}$	14280
		LTD	$-2.07526(8) \times 10^{-6}$	$+i 6.97192(8) \times 10^{-7}$	85

- This results shows have been implemented for several data points for tensor pentagons and hexagons.
- Integrals considering massive internal lines were computed numerically.
- The results using LTD are, in some cases, four order of magnitudes faster than SecDec.
- What about in a physical process ?

AT CROSS SECTION LEVEL

- A cross section is always finite at all orders in pQCD.
- Diagrammatically:

$$\sigma^{\text{LO}} = \text{[Diagram: LO cross section with a vertical cut line through the loop]}$$

$$\sigma^{\text{NLO}} = \text{[Diagram: NLO cross section with a vertical cut line through the loop and a red vertical line representing a real emission]} + \text{[Diagram: NLO cross section with a vertical cut line through the loop and a red diagonal line representing a virtual correction]}$$

- OBJECTIVE: Apply the LTD for matching the virtual and the real contributions at integrand level at NLO where the integrand should not have divergences.

IR REGULARISATION

- Let's define real and virtual cross sections as,

$$\tilde{\sigma}_{i,R} = \sigma_0^{-1} 2\text{Re} \int d\Phi_{1\rightarrow 3} \langle \mathcal{M}_{2r}^{(0)} | \mathcal{M}_{1r}^{(0)} \rangle \theta(y'_{jr} - y'_{ir})$$

$$\tilde{\sigma}_{i,V} = \sigma_0^{-1} 2\text{Re} \int d\Phi_{1\rightarrow 2} \langle \mathcal{M}^{(0)} | \mathcal{M}_i^{(1)} \rangle \theta(y'_{jr} - y'_{ir})$$

- where

$$\langle \mathcal{M}^{(0)} | \mathcal{M}_i^{(1)} \rangle = -g^4 s_{12} I_i \quad y'_{ir} = \frac{s_{12}}{s'_{ir}}$$

$$\langle \mathcal{M}_{2r}^{(0)} | \mathcal{M}_{1r}^{(0)} \rangle = g^4 s_{12} / (s'_{1r} s'_{2r})$$

- Momentum conservation: $p_1 + p_2 = p'_1 + p'_2 + p'_r$

- Claim: $\tilde{\sigma}_i = \tilde{\sigma}_{i,V} + \tilde{\sigma}_{i,R}$ allows a 4-dimensional representation at the integrand level.

- Building the mapping for the condition $y'_{1r} < y'_{2r}$:

$$p_r'^{\mu} = q_1^{\mu}$$

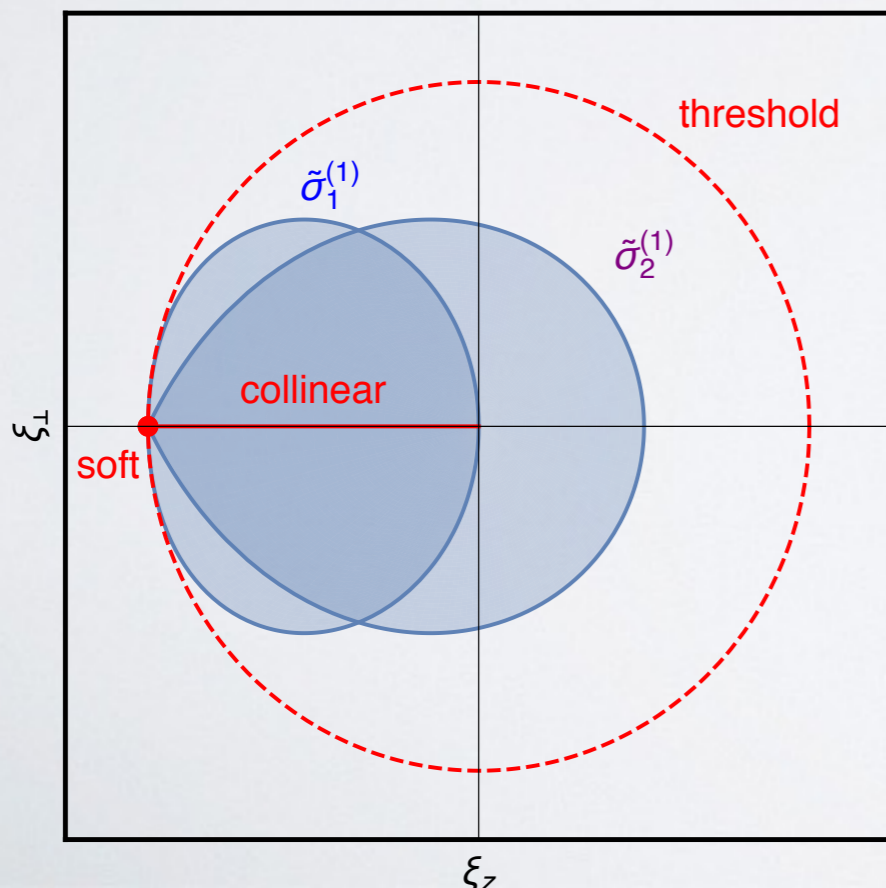
$$\alpha_1 = \frac{q_3^2}{2q_3 \cdot p_2}$$

$$p_1'^{\mu} = p_1^{\mu} - q_1^{\mu} + \alpha_1 p_2^{\mu}$$

$$q_1 = \ell + p_1$$

$$p_2'^{\mu} = (1 - \alpha_1) p_2^{\mu}$$

- and a similar mapping for $y'_{1r} > y'_{2r}$. The integral regions are



$$\tilde{\sigma}_1 = \mathcal{O}(\epsilon)$$

$$\tilde{\sigma}_2 = -c_\Gamma \frac{g^2 \pi^2}{s_{12} 6} + \mathcal{O}(\epsilon)$$

$$\bar{\sigma}_V = c_\Gamma \frac{g^2 \pi^2}{s_{12} 6} + \mathcal{O}(\epsilon)$$

UV RENORMALISATION

- UV renormalisation requires local cancellation of divergences.
- In general, counterterms are obtained by expanding the propagator around a UV propagator

$$G_F(q_i) = \frac{1}{q_{UV}^2 - \mu_{UV}^2 + i0} + \dots, \quad q_{UV} = \ell + k_{UV}$$

- For the bubble integral, the counterterm is

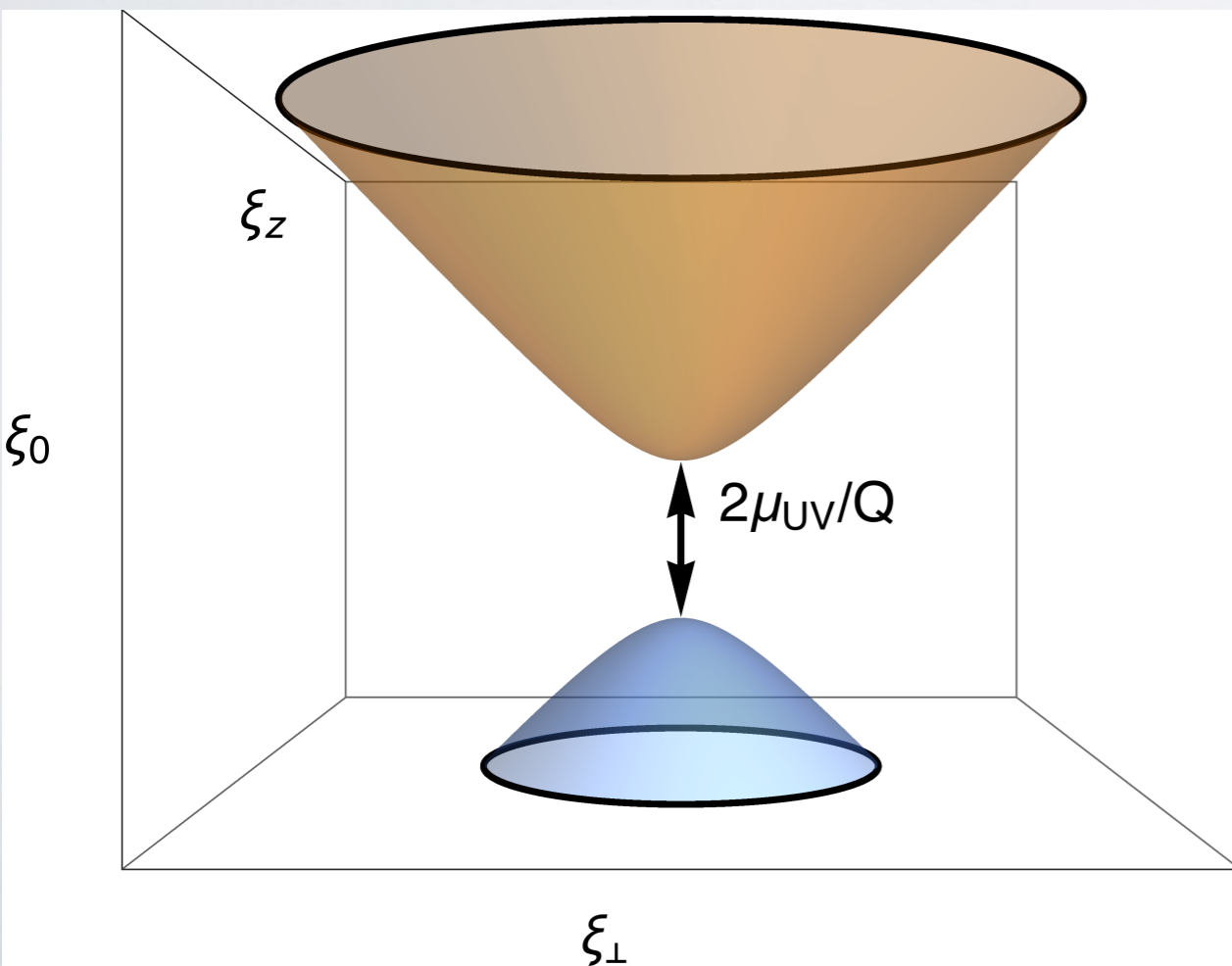
$$I_{UV}^{cnt} = \int_{\ell} \frac{1}{(q_{UV}^2 - \mu_{UV}^2 + i0)^2} \xrightarrow{\text{LTD}} I_{UV}^{cnt} = \int_{\ell} \frac{\tilde{\delta}(q_{UV})}{2(q_{UV,0}^{(+)})^2}$$

$$q_{UV,0}^{(+)} = \sqrt{\mathbf{q}_{UV}^2 + \mu_{UV}^2 - i0}$$

- 4 dimensional representation of the renormalised bubble integral is,

$$\begin{aligned}
 L^{(1,R)} &= L^{(1)}(p, -p) - I_{UV}^{cnt} \\
 &= -4 \int d[\xi]d[v] \left[\frac{\xi}{1 - 2\epsilon + i0} + \frac{\xi}{1 + 2\xi} + \frac{\xi^2}{2(\xi^2 + m_{UV}^2)^{3/2}} \right] \\
 &= \frac{1}{4\pi^2} \left[-\log \left(-\frac{p^2}{\mu_{UV}^2} - i0 \right) + 2 \right] + \mathcal{O}(\epsilon)
 \end{aligned}$$

- the integration regions corresponds to hyperboloids

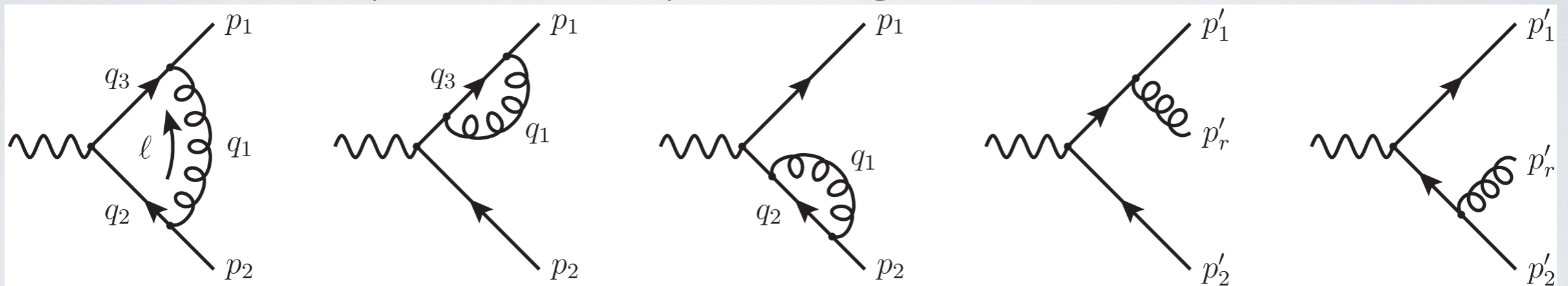


- Physical interpretation of renormalisation scale: Avoid the intersection of hyperboloids. Thus

$$\mu_{UV} = Q/2$$

$\gamma^* \rightarrow q\bar{q}$ AT NLO IN QCD

- In this well known process, the Feynman diagrams are



- where the process add more structure to the integrals. In general, virtual and real corrections have numerators.
- In this case, for the virtual correction is given by,

$$\langle \mathcal{M}_{q\bar{q}}^{(0)} | \mathcal{M}_{q\bar{q}}^{(1)} \rangle = g_S^2 C_F |\mathcal{M}_{q\bar{q}}^{(0)}|^2 \frac{4}{s_{12}} \int_{\ell} \left(\prod_{i=1}^3 G_F(q_i) \right) \times \epsilon \left[(2 + \epsilon)(q_2 \cdot p_1)(q_3 \cdot p_2) - \epsilon \left((q_2 \cdot p_2)(q_3 \cdot p_1) + \frac{s_{12}}{2}(q_2 \cdot q_3) \right) \right]$$

- and for the real correction is,

$$\sigma_R^{(1)} = \sigma^{(0)} \frac{(4\pi)^{\epsilon-2}}{\Gamma(1-\epsilon)} g_S^2 C_F \left(\frac{s_{12}}{\mu^2} \right)^{-\epsilon} \int_0^1 dy'_{1r} \int_0^{1-y'_{1r}} dy'_{2r} (y'_{1r} y'_{2r} y'_{12})^{-\epsilon} \\ \times \left[4 \left(\frac{y'_{12}}{y'_{1r} y'_{2r}} - \epsilon \right) + 2(1-\epsilon) \left(\frac{y'_{2r}}{y'_{1r}} + \frac{y'_{1r}}{y'_{2r}} \right) \right]$$

- Using DREG, the result is,

$$\sigma_V^{(1)} = \sigma^{(0)} c_\Gamma g_S^2 C_F \left(\frac{s_{12}}{\mu^2} \right)^{-\epsilon} \left[-\frac{4}{\epsilon^2} - \frac{6}{\epsilon} - 16 + 2\pi^2 + \mathcal{O}(\epsilon) \right]$$

$$\sigma_R^{(1)} = \sigma^{(0)} c_\Gamma g_S^2 C_F \left(\frac{s_{12}}{\mu^2} \right)^{-\epsilon} \left[\frac{4}{\epsilon^2} + \frac{6}{\epsilon} + 19 - 2\pi^2 + \mathcal{O}(\epsilon) \right]$$

- Then,

$$\sigma = \sigma^{(0)} \left(1 + 3C_F \frac{\alpha_S}{4\pi} + \mathcal{O}(\alpha_S^2) \right)$$

Remarks:

- There is no need of tensor reduction, no need of Gram determinants.
- Two point function of massless particles are usually ignored because is scaleless.
- In fact, this integral is zero because IR and UV poles cancels.
- In the LTD, there is an identification of IR and UV regions, therefore it has to be consider at the integrand level.

- Following the procedure described, it is possible to find 4-dimensional representations for the cross sections, resulting:

$$\tilde{\sigma}_1^{(1)} = \sigma^{(0)} \frac{\alpha_S}{4\pi} C_F \int_0^1 d\xi_{1,0} \int_0^{1/2} dv_1 4 \mathcal{R}_1(\xi_{1,0}, v_1) \left[2 (\xi_{1,0} - (1 - v_1)^{-1}) - \frac{\xi_{1,0}(1 - \xi_{1,0})}{(1 - (1 - v_1) \xi_{1,0})^2} \right],$$

$$\begin{aligned} \tilde{\sigma}_2^{(1)} = & \sigma^{(0)} \frac{\alpha_S}{4\pi} C_F \int_0^1 d\xi_{2,0} \int_0^1 dv_2 2 \mathcal{R}_2(\xi_{2,0}, v_2) (1 - v_2)^{-1} \left[\frac{2 v_2 \xi_{2,0} (\xi_{2,0}(1 - v_2) - 1)}{1 - \xi_{2,0}} \right. \\ & \left. - 1 + v_2 \xi_{2,0} + \frac{1}{1 - v_2 \xi_{2,0}} \left(\frac{(1 - \xi_{2,0})^2}{(1 - v_2 \xi_{2,0})^2} + \xi_{2,0}^2 \right) \right], \end{aligned}$$

$$\begin{aligned} \bar{\sigma}_V^{(1)} = & \sigma^{(0)} \frac{\alpha_S}{4\pi} C_F \int_0^\infty d\xi \int_0^1 dv \left\{ -2 (1 - \mathcal{R}_1(\xi, v)) v^{-1} (1 - v)^{-1} \frac{\xi^2 (1 - 2v)^2 + 1}{\sqrt{(1 + \xi)^2 - 4v\xi}} \right. \\ & + 2 (1 - \mathcal{R}_2(\xi, v)) (1 - v)^{-1} \left[2 v \xi (\xi(1 - v) - 1) \left(\frac{1}{1 - \xi + i0} + i\pi\delta(1 - \xi) \right) - 1 + v \xi \right] \\ & + 2 v^{-1} \left(\frac{\xi(1 - v)(\xi(1 - 2v) - 1)}{1 + \xi} + 1 \right) - \frac{(1 - 2v) \xi^3 (12 - 7m_{UV}^2 - 4\xi^2)}{(\xi^2 + m_{UV}^2)^{5/2}} \\ & \left. - \frac{2 \xi^2 (m_{UV}^2 + 4\xi^2(1 - 6v(1 - v)))}{(\xi^2 + m_{UV}^2)^{5/2}} \right\}, \end{aligned}$$

- These expressions can be integrated analytically, resulting:

$$\tilde{\sigma}_1^{(1)} = \sigma^{(0)} \frac{\alpha_S}{4\pi} C_F (19 - 32 \log(2)),$$

$$\tilde{\sigma}_2^{(1)} = \sigma^{(0)} \frac{\alpha_S}{4\pi} C_F \left(-\frac{11}{2} + 8 \log(2) - \frac{\pi^2}{3} \right),$$

$$\bar{\sigma}_V^{(1)} = \sigma^{(0)} \frac{\alpha_S}{4\pi} C_F \left(-\frac{21}{2} + 24 \log(2) + \frac{\pi^2}{3} \right).$$

- Thus: $\tilde{\sigma}_1^{(1)} + \tilde{\sigma}_2^{(1)} + \bar{\sigma}_V^{(1)} = \sigma^{(0)} 3C_F \frac{\alpha_S}{4\pi}$
- Computation of multi-legs and NNLO corrections are doable within the LTD.

CONCLUSIONS

- New methods for computing higher order corrections are needed for upcoming LHC observables.
- Mapping of momenta between real and virtual corrections permits to cancel soft and final-state collinear singularities.
- Fully local cancellation of IR and UV divergences through the LTD.
- LTD allows to build an algorithm for computing 4-dimensional representations of NLO cross sections.
- Extension of the LTD at NNLO and multi-leg processes is on the way.

THANKS...
